it is that of the so-called Type II atoms we considered in Chapter 4, in our discussion of quantum beats. Excite the atom to its upper level a and wait for a long time, until the decay has certainly taken place. We can write the state of the atom–photon system after the decay is over as

$$\psi = \frac{1}{\sqrt{2}}[\phi_h \omega_h + \phi_g \omega_g] \tag{8.12}$$

Here ϕ represents the atom's state and ω that of the electromagnetic field. The reader will recognize Equation (8.12) as describing an entanglement: if, after the decay, the atom is left in state h, then a photon of energy ω_h had been emitted; and if the atom is in state g, then the photon's energy was ω_g.

Let us now *measure* the state of the atom. To be specific, our measuring apparatus is designed to determine the atom's energy. The result will either be E_h or E_g. Whichever result we get collapses the wave function: if we measure E_h the state becomes

$$\psi = \phi_h \omega_h \tag{8.13}$$

and if we measure E_g the state becomes

$$\psi = \phi_g \omega_g \tag{8.14}$$

The point we wish to focus on here is that *each of these states contains a photon of well-defined energy*.

But Jaynes then goes on to describe a different sort of measuring apparatus, one that will force the photons to be of undefined energy. He begins by defining a particular linear superposition of atomic and field states:

$$\begin{aligned}
\phi_+ &\equiv \frac{1}{\sqrt{2}}[\phi_g + e^{i\theta}\phi_h] \\
\phi_- &\equiv \frac{1}{\sqrt{2}}[\phi_g - e^{i\theta}\phi_h] \\
\omega_+ &\equiv \frac{1}{\sqrt{2}}[\omega_g + \omega_h] \\
\omega_- &\equiv \frac{1}{\sqrt{2}}[\omega_g - \omega_h]
\end{aligned} \tag{8.15}$$

where θ is a constant. If Equations (8.15) are substituted in Equation (8.12), we see that the entangled state after the decay can also be written as

$$\psi = \frac{1}{\sqrt{2}}[\phi_+ \omega_+ + \phi_- \omega_-] \tag{8.16}$$

Jaynes then describes a second type of measuring apparatus, one that determines not whether the atom is in the state ϕ_h or ϕ_g, but whether it is in state ϕ_+ or ϕ_-. It turns out that this new apparatus is only a slight variation on the first. The difference merely consists in applying to the atom a pulse of electromagnetic radiation, of a precisely specified intensity and duration,

just before measuring its energy. It turns out that, if the atom's state before the pulse is ϕ_+, then after the pulse it will be ϕ_g; and if the atom's state had been ϕ_-, then afterwards it will be ϕ_h. The apparatus then goes on simply to measure the atom's energy in the usual way.

Suppose that, upon making this second sort of measurement, we find the atom's state to be ϕ_g. This means that, prior to the measurement, the joint atom–field state had been

$$\psi = \phi_+ \omega_+ \tag{8.17}$$

Conversely, if we find that the atom's state is ϕ_h, then prior to the measurement the state had been

$$\psi = \phi_- \omega_- \tag{8.18}$$

As always, the measurement collapses the wave function. But notice that *in this case, the state to which the collapse leads, if expanded in energy eigenstates, contains a photon whose energy is a superposition of two terms.*

And finally, notice that our measurement of the atom's state can be delayed indefinitely. We could do it a year after the decay. Thus, Jaynes concludes, it is not correct to say that a given decay produces a photon with definite properties. Rather, we must accept the fact that these properties depend on the sort of measurement we elect to make—and that this measurement can be made long after the decay has happened.

We emphasize that the distinction between these two states is not only of conceptual interest. It also has a clear experimental signature: the existence or nonexistence of the quantum beats we discussed in Chapter 4. Indeed, an experiment illustrating this remarkable situation has actually been performed. The delayed-choice experiment of Hellmuth et al.,[4] which we described in Chapter 2, has been performed in a mode in which these beats were made to appear and disappear by choosing, significantly after the decay had taken place, which sort of measurement to perform.

Jaynes's comment on this state of affairs is worth quoting:[3]

> From this, it is pretty clear why present quantum theory not only does not use—it does not even dare to mention—the notion of a "real physical situation." Defenders of the theory say that this notion is philosophically naive, a throwback to outmoded ways of thinking, and that recognition of this constitutes deep new wisdom about the nature of human knowledge. I say that it constitutes a violent irrationality, that somewhere in this theory the distinction between reality and our knowledge of reality has become lost, and the result has more the character of medieval necromancy than science.

The Quantum Zeno Effect As the old maxim goes, a watched pot never boils. In the quantum world, this is not a joke. The act of observing a process

G. Greenstein, A. Zajonc, "The quantum challenge" (2005)

can slow that process, and in the limit of continuous measurement, can completely stop it.

The effect is sometimes known as the quantum Zeno effect, named by Misra and Sudarshan[5] after Zeno's famous paradoxes that appear to show that motion is impossible. The idea first arose in connection with the decay of an unstable state. It was argued that, if one were to prepare an atom in an unstable excited state, and then repeatedly observe it to see if it had decayed, the observations would slow the decay. Indeed, Misra and Sudarshan's calculations showed that, as the number of observations increased without limit, the state was predicted *never* to decay.

Although this calculation referred to the spontaneous decay from an unstable state, the same effect should exist for induced transitions. An experiment illustrating this phenomenon has recently been performed by Itano, Heinzein, Bollinger and Wineland.[6] The process Itano and colleagues studied is the excitation of an atom by light. As we discussed above (Figure 8–4), an electromagnetic wave is capable of raising an atom from its ground state to an excited state with certainty if an appropriate electromagnetic pulse is applied. While quantum theory cannot predict just when any individual atom makes the upward jump, it does predict that, after the time T_{ex} illustrated in Figure 8–4, the transition is sure to have happened. In their experiment, Itano et al. showed that this transition probability was reduced if they looked to see whether the transition had in fact occurred.

It is not hard to understand how this remarkable effect comes about. Let us consider an atom with a ground state ϕ_{gd} and excited state ϕ_{ex}. We wrote the atomic state in Equation (8.3), where α_{gd} is the coefficient of the ground state and α_{ex} that of the excited state. These coe0fficients are graphed in Figure 8–5. We see that initially α_{gd} smoothly drops, while α_{ex} correspondingly rises.

The initial state is $\alpha_{gd} = 1$ and $\alpha_{ex} = 0$. Consider the state after a short time t, where by "short" we mean a time less than that required to make the transition: $t < T_{ex}$. At this time, the coefficient of the ground state has dropped somewhat, and that of the excited state has risen.

We emphasize, however, that this is the state in the absence of a measurement. Let us now ask what happens if we *do* make a measurement. Suppose the measurement finds the atom to be still in its ground state. This collapses the wave function to

$$\psi_{\text{after measurement}} = \phi_{gd} \tag{8.19}$$

But this is just the initial state. The collapse of the wave function has "re-set the clock" from t to 0. It is as if the time interval from 0 to t had simply never happened. Thus we see that in this case the act of observation has slowed the decay rate.

Conversely, if the measurement reveals the atom to be in the excited state, the collapse leads to this state, in which case the measurement has

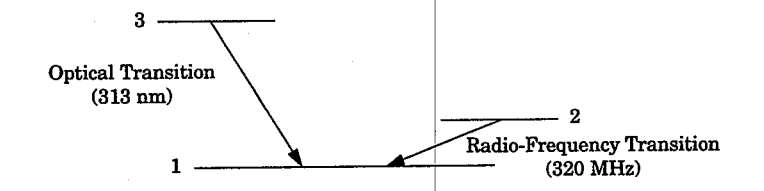

Figure 8–9 *Quantum Zeno Experiment* of Itano et al.[6] made use of the indicated transitions.

hastened the decay. But if the measurements are frequent, t will be far less than T_{ex}, and the chances of this happening are small. We will shortly show that the net effect is a slowing of the decay.

Let us pursue these ideas in more detail. Working at the National Institute of Standards and Technology, Itano and colleagues made use of new techniques that allowed small numbers of ions to be trapped in an electromagnetic field, far away from the walls of their apparatus. These ions hovered in space, where they were slowed and then manipulated by a sequence of optical and radio-frequency fields. (The experiment by Chu et al., which we described in Chapter 3, used similar experimental methods.) The ions were of beryllium, only three energy levels of which are of interest: we label them 1, 2, and 3 and indicate them in Figure 8–9. Levels 1 and 2 are very close together, and are separated by only 320 MHz, a radio frequency. The transition from 1 to 3, on the other hand, is an allowed optical transition, with a wavelength of 313 nm.

The two states 1 and 2 were connected by a strong applied radio-frequency field, which drove the transition so rapidly that spontaneous decay from 2 to 1 was negligible, and only the stimulated transitions were of significance. As we have seen, under such circumstances the ions cycle between states 1 and 2 at the Rabi frequency Ω. This implies that the probability of finding the ion in the lower state is

$$P_1(t) = \cos^2(\Omega t/2) \tag{8.20}$$

and that of finding it in the upper state is

$$P_2(t) = \sin^2(\Omega t/2) \tag{8.21}$$

These are simply the quantities sketched in Figure 8–4.

Once again, we emphasize that this is only true if one does not measure the system. If we do observe it, the observation collapses the state to either 1 or 2. In the Itano experiment, the measurement was performed by applying a short probe pulse, this time an optical one precisely tuned to a different

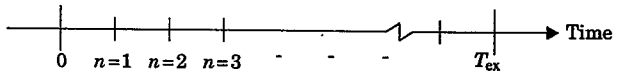

Figure 8–10 *Time Line* indicating T_{ex}, the time required for the atom to make a transition if not observed, and the n observations made by Itano et al.[6] which delayed the transition.

transition, that between 1 and 3. It was adjusted to drive the transition with 100% certainty. Thus, had the ions been in the state 1 prior to this pulse, they would be in 3 after it. Conversely, had they been in state 2 prior to the pulse, they would still be in 2 after it.

The final step in Itano et al.'s measurement process was then to wait and search for *the photon emitted when the ion decayed from level 3 back to level 1*. Since this photon could only be emitted had the ion been in the state 1 prior to the pulse, its presence or absence constituted the measurement of the state.

We emphasize that the transition under consideration was that between 1 and 2; the observations of whether it had happened were made by studying a second transition, that between 1 and 3. We now need to consider how these observations affect the probability of induced transitions between states 1 and 2.

First, let us find the time T_{ex}, which is the time it takes for the radio-frequency field to move the ions with 100% certainty from state 1 to 2. Because it is just $T_{ex} = \pi/\Omega$, a pulse of this duration is called a π-pulse. Putting $t = T_{ex} = \pi/\Omega$ in Equations (8.20)–(8.21), we see that after the time T_{ex}, $P_1(T_{ex}) = 0$ and $P_2(T_{ex}) = 1$, as expected. During the time interval from $t = 0$ to $t = T_{ex}$, Itano et al. then made a series of n measurements of the ion's state, separated in time by $\Delta t = T_{ex}/n = \pi/n\Omega$. Figure 8–10 shows the interval T_{ex} divided up into n such subintervals, each of length Δt.

We now need to evaluate

- the probability for a transition in a subinterval Δt;
- the probability for no transition in a subinterval Δt.

At this point a potential difficulty arises. If the probabilities given by Equations (8.20)–(8.21) were linear functions of the time, then the transition *rate* would be constant in time. But Equations (8.20)–(8.21) are not linear. This means that the rate varies with time, and the probability of transition in any particular subinterval will depend on just *which* subinterval we are considering. Here the collapse hypothesis intervenes to simplify the problem! Since Itano et al. are measuring the ion's state at the beginning of each subinterval, the collapse process "re-sets the clock" at each measurement—to $t = 0$ if the result of the measurement is level 1, and to $t = T_{ex}$ if the result is level 2. Thus we can use Equations (8.20)–(8.21) without asking

which subinterval they are being applied to. They show that the probability of the ion making a transition to 2 during the time Δt, if it was in level 1 at the beginning of this interval, is

$$P_2(\Delta t) = \sin^2\left(\frac{\pi}{2n}\right) = \left(\frac{1}{2}\right)\left[1 - \cos\left(\frac{\pi}{2n}\right)\right] \tag{8.22}$$

and the probability of it staying in level 1 during Δt is

$$p_1(\Delta t) = \cos^2\left(\frac{\pi}{2n}\right) = \left(\frac{1}{2}\right)\left[1 + \cos\left(\frac{\pi}{2n}\right)\right] \tag{8.23}$$

If, on the other hand, the ion was in level 2 at the beginning of the subinterval, then the probabilities are given by Equations (8.20)–(8.21) evaluated at $T_{ex} + \Delta t = (\pi/2)[1 + (1/n)]$.

We now evaluate the probability of transition from 1 to 2 after *the entire* interval T_{ex} has passed, having made the n measurements in that time. To see how the calculation is done, begin with the particularly simple case $n = 2$: only two observations are made, one at $t = T_{ex}/2$, and the other at $t = T_{ex}$. There are, in this case, only two subintervals, and there are only two ways in which the ion, having started in level 1, could end up in level 2 at the end of the time T_{ex}:

(a) a transition occurs in the first subinterval, and no transition occurs in the second;
(b) no transition occurs in the first subinterval, but one does happen in the second.

We begin with (a). The probability of a transition in the first subinterval is just $P_2(T_{ex}/2)$. The probability of no transition in the second, given that the state was 2 at the beginning of this subinterval, is given by $P_2(T_{ex} + T_{ex}/2)$. The probability of the course of events (a) is then

$$P_a = P_2\left(\frac{T_{ex}}{2}\right)P_2\left(T_{ex} + \frac{T_{ex}}{2}\right) = \left(\frac{1}{2}\right)\left(\frac{1}{2}\right) = \frac{1}{4} \tag{8.24}$$

Similarly, the probability P_b for the second course of events turns out to be just the same product in reverse order, and therefore is likewise $\frac{1}{4}$. The overall probability of finding the ion in level 2 after 2 measurements in the time interval T_{ex} is therefore

$$P = P_a + P_b = \tfrac{1}{2} \tag{8.25}$$

Notice that, in the absence of measurements, this probability would have been 1: *the act of observing the ions twice has cut the probability of transition in half.*

The calculation can be extended to greater numbers of observations in a similar manner. The following general expression can be derived for the

probability of finding the ion in level 2 after a time T_{ex} given n equally spaced measurements:

$$P = \left(\frac{1}{2}\right)\left[1 - \cos^n\left(\frac{\pi}{n}\right)\right] \tag{8.26}$$

This probability is what Itano et al. compared to their experimental data.

In their experiment, about 5000 beryllium ions were loaded into the trap, cooled to about 0.25 K, and prepared in state 1. The radio-frequency field was then turned on for 0.256 s, with an intensity adjusted to make it exactly a π-pulse. If no intervening measurements were made ($n = 1$), then at the end of the 0.256-s interval, all the ions would be in the state 2. During the radio-frequency pulse, however, n short 313-nm probe pulses were also applied, with n taking on values 1, 2, 4, 8, 16, 32, or 64. The resulting 313-nm decay photons were searched for: these comprised the measurements of the state of the ions. After suitable calibration, Itano et al. were able to compare their experimental results with the predictions of Equation (8.26). Figure 8–11 shows a bar graph of their data for the transition probability from levels 1 to 2 as a function of the number of their measurements n; it also gives the theoretical predictions. The

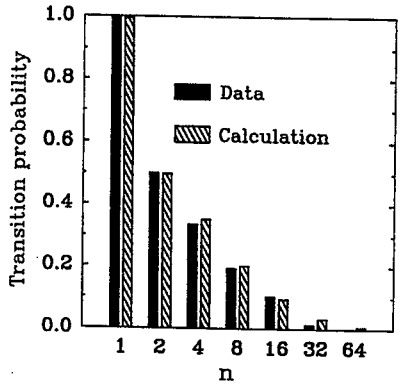

Figure 8–11 *Results of the Quantum Zeno Experiment.* The probability of having made a transition after a time T_{ex} as a function of the number of intermediate observations n. The decrease of the transition probability with n is the quantum Zeno effect. Agreement of the observations (solid bars) and theory (hatched bars) is excellent. SOURCE: Reproduced with permission from W.M. Itano, D.J. Heinzen, J.J. Bollinger and D.J. Wineland, "Quantum Zeno effect," *Phys. Rev. A*, vol. 41, p. 2295 (1990), published by The American Physical Society.

decreasing probability with increasing n is the quantum Zeno effect. The agreement between theory and experiment is excellent.

The experiment is a beautiful one and its results are unambiguous. Unfortunately, however, its interpretation is not. Following Itano et al.'s own description, we have used the language of the collapse of the wave function in analyzing their experiment. Other physicists, however, have argued that this is unnecessary, and they have performed alternative analyses, successfully predicting its results *without resorting to the collapse process*. So at this point, all we can say is that the quantum Zeno effect is real, but its interpretation in support of the collapse hypothesis remains only one option among many.

This lack of clarity is characteristic of the problem of collapse. In every other chapter of this book, we have been able to achieve considerable insight into the details of the theory and the corresponding experiments. The various quantum phenomena we have studied challenge our conventional understanding of the world—but the formalism and the experimental data are relatively straightforward, and though detailed interpretations may vary, the overall implications are generally agreed upon. As soon as we encounter the problem of measurement, however, this clarity gives way. The best we can hope for is to refine our definition of the problem itself. In this way, we can at least become increasingly clear about the source of our confusion.

8.3 Attempts to Solve the Measurement Problem

The measurement problem described in the first section of this chapter has received much attention. We turn now to a description of some of the many attempts that have been made to solve it. We caution the reader that there is no general agreement as to where the actual solution lies, so our discussion will not lead to any definite conclusion.

Small Detectors and Big Detectors: Decoherence Return to our analysis of the infinite regress that develops when we attempt to describe a measurement. Recall our comment that, in going from Equation (8.5) to Equation (8.6), an important new element has entered the situation: *we made a transition from microscopic to macroscopic.* Recall also from the previous chapter that large objects, unless they are of a very special sort, are subject to the process of decoherence. A number of workers in the field have argued that *this solves the measurement problem.* Their claim is that decoherence does away with the need for the projection postulate. We turn now to this claim.

At the close of our discussion of decoherence, we summarized its essential points (Section 7.5). We now repeat that summary, but with one change—everywhere the word "system" appeared before, we now write "macroscopic detector":

> [The essential elements of decoherence are] as follows. (I) The environment in which any macroscopic detector is embedded is constantly and irregularly fluctuating. (II) If a macroscopic detector is

efficient completion of the second step, and that this arrangement allows accumulation of what would normally be reaction intermediates. In the case of telomerase RNA, however, one of these intermediates is the final, processed product that functions as part of the telomerase enzyme. It is therefore the incomplete function of the spliceosome — as measured by mRNA-production standards — that is needed for the formation of telomerase RNA.

Telomerase activity is essential for long-term cell proliferation — including stem-cell renewal and cancer-cell immortalization — and increased telomerase activity can delay ageing in cancer-resistant mice[2,8]. So it will be of interest to know whether Box and colleagues' results[3] in *S. pombe* apply to other organisms.

Conceivably, modulation of spliceosome activity — such as changes in the efficiency of the second catalytic step and of the release of splicing intermediates from the spliceosome complex — could control telomerase function in organisms in which telomerase RNA follows this processing route. Polyadenylated and/or longer telomerase-gene transcripts have been identified in other species, including humans[9,10], but whether the spliceosome plays a part in the synthesis of telomeric RNA in these organisms remains unknown.

A notable insight comes from Box and colleagues' observation that the spliceosome can generate the proper 3′ end of telomerase RNA. It could be that other RNA molecules can similarly exploit this incomplete activity of the spliceosome to generate alternative transcript ends. If so, the expanding world of non-coding RNAs, many of which contain introns, could offer a large inventory of substrates for diversification of the cellular pool of RNA transcripts, adding to the complexity of the still largely hidden genetic program of our genomes[11]. ■

Sophie Bonnal and Juan Valcárcel are at the Centre de Regulació Genòmica and Universitat Pompeu Fabra, Barcelona, Spain. Juan Valcárcel is also at the Institució Catalana de Recerca i Estudis Avançats, Dr. Aiguader 88, 08003 Barcelona, Spain.
e-mail: juan.valcarcel@crg.es

1. www.gateworld.net/atlantis/s4/transcripts/419.shtml
2. Blasco, M. A. *Nature Chem. Biol.* **3,** 640–648 (2007).
3. Box, J. A., Bunch, J. T., Tang, W. & Baumann, P. *Nature* **456,** 910–914 (2008).
4. Blackburn, E. H. *FEBS Lett.* **579,** 859–862 (2005).
5. Leonardi, J., Box, J. A., Bunch, J. T. & Baumann, P. *Nature Struct. Mol. Biol.* **15,** 26–33 (2008).
6. Webb, C. J. & Zakian, V. A. *Nature Struct. Mol. Biol.* **15,** 34–42 (2008).
7. Will, C. L. & Lührmann, R. in *The RNA World* 3rd edn (eds Gesteland, R. F., Cech, T. R. & Atkins, J. F.) 369–400 (Cold Spring Harbor Laboratory Press, 2005).
8. Tomás-Loba, A. *et al. Cell* **135,** 609–622 (2008).
9. Chapon, C., Cech, T. R. & Zaug, A. J. *RNA* **3,** 1337–1351 (1997).
10. Fu, D. & Collins, K. *Mol. Cell* **11,** 1361–1372 (2003).
11. Mattick, J. S. & Makunin, I. V. *Hum. Mol. Genet.* **15,** R17–R29 (2006).

QUANTUM PHYSICS

Don't look now

Alexei Ourjoumtsev

Before picking up the phone and calling a technician to fix a faulty microwave oven, there are always a few simple things one should check. So far, "stop looking at it" has not been part of the checklist.

For people with a special kind of imagination, microwave oven manuals contain warnings such as "do not use it to dry animals or as a storage place for books"[1]. For everyone else, the daily operation is basic: close the door, set the time and press the start button. Now, physicists might be tempted to add "and don't look inside or it won't work". Writing in *Physical Review Letters*, Bernu *et al.*[2] show that the build-up of a microwave inside a resonator can be blocked by just 'watching' it without absorbing the wave's energy. The edge of a very strange quantum world is now one step closer to everyday life.

Nature states firmly that information has a price. The lowest, non-negotiable one is set by quantum physics: measuring something always disturbs something else. Usually, this disturbance goes unnoticed. To detect a microwave, it is generally converted into an electric current by an antenna, or into the heat that cooks your food, so the wave is not only perturbed but destroyed. But even if you were an outstanding experimentalist and you could measure the microwave's intensity at the ultimate quantum level without absorbing a single photon, you would still leave your fingerprint by making its phase completely random. Instead of regular oscillations, the wave would make a sudden jump. This is exactly what happened in Bernu and colleagues' experiment[2].

Start injecting an empty cavity with a resonant wave: it builds up and, after a short time (say, a tenth of a second), its amplitude reaches a value α. Let's see this again in slow motion. First, a small wavelet comes in. At resonance, it makes an integer number of oscillations during a cavity round-trip. Therefore, it remains in phase with the next incoming wavelet, and they simply add up. And so on. After 100 milliseconds, the wave in the cavity is made of N identical wavelets, all oscillating in phase with the same amplitude α/N. In a sense, the intracavity field makes N steps each with a length α/N in a direction defined by the phase of the wavelets (Fig. 1a).

However, if one now repeats the same procedure but measures the number of photons after each wavelet injection, their phases will become totally random: the field will still 'walk' by steps of α/N, but in completely random directions (Fig. 1b). As in a usual diffusion phenomenon, N steps will typically result in an amplitude of $(\alpha/N) \times \sqrt{N} = \alpha/\sqrt{N}$, so the final intensity will be only α^2/N instead of α^2. If measured more and more often, this attenuation factor $1/N$ will become smaller and smaller, and eventually the resonator will simply become empty. This so-called quantum Zeno effect, which prevents a system from evolving while observed, has been convincingly demonstrated before, but usually in conjunction with other quantum effects, such as Bose–Einstein condensation or quantum tunnelling[3–8]. The object of interest was never as simple and classical as the intensity of a microwave in a cavity.

For Bernu and colleagues, the key to success was an incredibly good microwave resonator. Indeed, to measure the exact number of photons, everything they interact with must be under absolute control. Photons must obey two commandments: "You shall not appear in the resonator unless I send you", and "You shall not leave it before I'm done with measuring you". For Bernu *et al.* this meant building a cavity in which tightly confined photons could bounce between two superconducting mirrors about 1 billion times, cooled to a temperature of 0.8 kelvin to prevent undesired thermal photons from appearing. In addition, keeping the cavity on resonance required its frequency to be stabilized with a relative precision of about 10^{-11}. All this led to a clear, fivefold microwave-intensity reduction after a 100-millisecond experimental sequence of alternating-field injections and photon counting.

But how can one count photons without destroying them? In physics, an old trick to measure a weak signal with low disturbance is to observe how it affects the motion of a pendulum. Just choose the right one. Back in 1846, a pendulum the size of a planet (Uranus) was used to detect Neptune. Five years later, just next door to the Ecole Normale Supérieure in Paris, where Bernu and co-workers performed their experiments, Léon Foucault used a smaller, yet still impressive, pendulum to demonstrate the rotation of the Earth.

Bernu *et al.* downsized the pendulum to the atomic scale. They excited individual rubidium atoms to 'Rydberg' states, making an electron oscillate between two orbits far away from the nucleus. These atoms acted as light-sensitive atomic clocks, the 'time' being given by the phase of their oscillations. When they were sent across the resonator, the hands

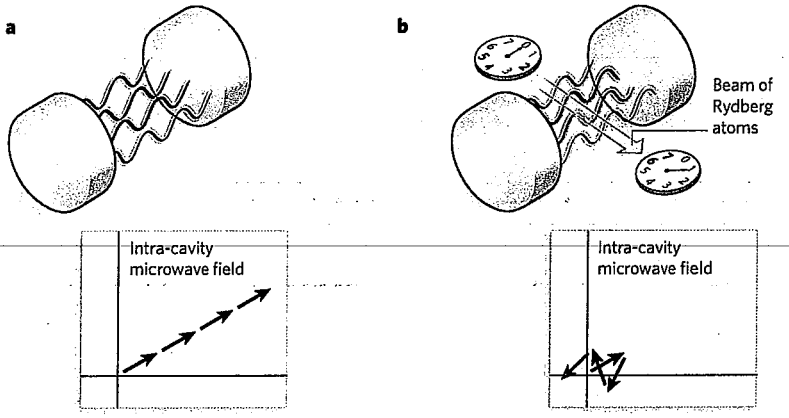

Figure 1 | Non-destructive intensity measurements. **a**, The build-up of a resonant wave in an empty cavity corresponds to the consecutive injection of N identical wavelets, all oscillating with the same amplitude α/N and the same phase φ. They can be represented by small vectors with a length α/N and an angle φ, which respectively define the length and the direction of elementary 'steps' made by the total intra-cavity field. A resonant field 'walks' away from zero always in the same direction and acquires an amplitude α ($(\alpha/N) \times N$) after N steps. **b**, Bernu *et al.*[2] use a beam of rubidium Rydberg atoms, which act as a light-sensitive atomic clock, to measure non-destructively the number of photons in the cavity between each wavelet injection. Owing to the quantum back-action of this measurement, the phases of the wavelets become random. The intra-cavity microwave field undergoes a random two-dimensional walk, and after N measurements its average amplitude is only $(\alpha/N) \times \sqrt{N} = \alpha/\sqrt{N}$. Increasing N decreases this amplitude, and therefore the final intensity of the field.

of these clocks were shifted by the microwave photons, each photon adding a shift of 45°. The electronic state of the atoms was measured outside the cavity by ionizing the most excited ones, and the electric current created was amplified to become measurable. This last, 'destructive' part of the measurement affected only the atomic probe, leaving the microwave photons intact.

The Zeno effect cannot prevent the irreversible decay of the microwave's intensity. In an oven with a typical power of 1 kilowatt, one microwave photon is lost every 10^{-27} seconds, much too fast to count the photons left inside the resonator. There is thus no need to rewrite the user manual. But Bernu and colleagues' demonstration that the coherent evolution of a system can be 'frozen' by non-destructive measurements is a significant step forward for quantum control. For instance, one could continuously modify the way of measuring the system to bring it into exotic quantum states that cannot be prepared otherwise. But above all, this work is one of an impressive series[9–11], demonstrating three essential qualities of Bernu and co-workers: expertise, rigour and a love of fundamental physics. ■

Alexei Ourjoumtsev is at the Max Planck Institute for Quantum Optics, Hans-Kopfermann Strasse 1, Garching D-85748, Germany.
e-mail: alexei.ourjoumtsev@mpq.mpg.de

1. Daewoo KOC-870T instruction manual, page b (1999).
2. Bernu, J. *et al. Phys. Rev. Lett.* **101,** 180402 (2008).
3. Nagels, B., Hermans, L. J. F. & Chapovsky, P. L. *Phys. Rev. Lett.* **79,** 3097 (1997).
4. Itano, W. M., Heinzen, D. J., Bollinger, J. J. & Wineland, D. J. *Phys. Rev. A* **41,** 2295 (1990).
5. Balzer, C., Huesmann, R., Neuhauser, W. & Toschek, P. *Opt. Commun.* **180,** 115–120 (2000).
6. Streed, E. W. *et al. Phys. Rev. Lett.* **97,** 260402 (2006).
7. Kwiat, P. G. *et al. Phys. Rev. Lett.* **83,** 4725 (1999).
8. Hosten, O. *et al. Nature* **439,** 949–952 (2006).
9. Gleyzes, S. *et al. Nature* **446,** 297–300 (2007).
10. Guerlin, C. *et al. Nature* **448,** 889–893 (2007).
11. Deléglise, S. *et al. Nature* **455,** 510–514 (2008).

CIRCADIAN CLOCKS

Tips from the tip of the iceberg

Fred W. Turek

Daily remodelling of histone proteins underlies interactions between circadian clock genes and metabolic genes. This regulatory mechanism could be widespread, affecting other physiological processes.

If you monitor the precise daily onset of wheel-running behaviour in a mouse kept in an environment devoid of time cues, you can predict that, tomorrow, the animal will start running 23.7 hours — not 23.6 hours, not 23.8 hours — from when it started today. This is because, in organisms as diverse as bread mould, fruitflies, mice and humans, a central circadian clock program coordinates multiple behavioural and physiological processes, including movement, sleep and energy balance, on a daily basis, even when the organism is removed from all external time cues such as the daily light–dark cycle. How such circadian processes are regulated at a molecular level has long fascinated scientists. On page 997 of this issue, Alenghat *et al.*[1] provide a clue: activation of an enzyme that is involved in chemical modification of chromatin (complexes of DNA and histone proteins) is a central point in the regulation of circadian metabolic processes.

Since the 1970s, studies on the anatomy, neurobiology and function of the mammalian circadian clock have focused on a brain region called the suprachiasmatic nucleus, which has a central role in regulating most, if not all, daily behavioural, physiological and cellular rhythms[2]. It emerged that numerous canonical circadian clock genes (such as *Clock, Pers, BMAL1* and *Crys*) are expressed in many central and peripheral tissues, and that, *in vitro*, the molecular clock could regulate the diurnal transcription of at least 10% of the genes in any given tissue[3]. These findings led to the realization that the circadian clock is not just central to the overall temporal regulation of behaviour and physiology, but that it perhaps also has a key role in the regulation of many cellular pathways and networks in various tissues and organs.

Particular attention was paid to how the molecular circadian clock affects processes related to energy homeostasis. There were two main reasons for this. First, mutation of a key circadian gene, *Clock*, leads to obesity and metabolic syndrome — a combination of disorders that increases the risk of diabetes and heart disease[4]. Second, several genes involved in metabolism, including those mediating the formation of fatty tissue and carbohydrate metabolism (such as *Rev-erbα, Rorα* and *Pparα*), show reciprocal regulation with core circadian clock genes[5].

Alenghat and colleagues' results[1] link these 'chronometabolic' molecular interactions to the cyclic regulation of chromatin through histone acetylation. They show that a specific genetic disruption of the interaction between the nuclear receptor co-repressor 1 (Ncor1) and the chromatin-modifying enzyme histone deacetylase 3 (Hdac3), which is activated by Ncor1, leads to aberrant regulation of clock genes and abnormal circadian behaviour. In turn, the oscillatory expression pattern of several metabolic genes is disrupted, leading to alterations in energy balance. The authors find that mice with loss of function of the Ncor1–Hdac3 complex are leaner than normal,

1. Payre, F., Vincent, A. & Carreno, S. *Nature* **400**, 271–275 (1999).
2. Tsuda, M. *et al. Nature* **400**, 276–280 (1999).
3. Lin, X. & Perrimon, N. *Nature* **400**, 281–284 (1999).
4. Meneghini, M. D. *et al. Nature* **399**, 793–797 (1999).
5. Ishitani, T. *et al. Nature* **399**, 798–802 (1999).
6. Gat, U., DasGupta, R., Degenstein, L. & Fuchs, E. *Cell* **95**, 605–614 (1998).
7. Wodarz, A. & Nusse, R. *Annu. Rev. Cell Dev. Biol.* **14**, 59–88 (1998).
8. Polakis, P. *Curr. Opin. Genet. Dev.* **9**, 15–21 (1999).
9. Fagotto, F. *et al. J. Cell Biol.* **145**, 741–756 (1999).
10. Kishida, S. *et al. Mol. Cell. Biol.* **19**, 4414–4422 (1999).
11. Smalley, M. J. *et al. EMBO J.* **18**, 2823–2835 (1999).
12. Maniatis, T. *Genes Dev.* **13**, 505–510 (1999).
13. Eastman, Q. & Grosschedl, R. *Curr. Opin. Cell Biol.* **11**, 233–240 (1999).
14. Gallet, A. *et al. EMBO J.* **18**, 2208–2217 (1999).
15. Shulman, J. M., Perrimon, N. & Axelrod, J. D. *Trends Genet.* **14**, 452–458 (1998).
16. Schlesinger, A., Shelton, C. A., Maloof, J. N., Meneghini, M. & Bowerman, B. *Genes Dev.* (in the press).
17. Rocheleau, C. E. *et al. Cell* **97**, 717–726 (1999).
18. Novak, A. *et al. Proc. Natl Acad. Sci. USA* **95**, 4374–4379 (1998).

Quantum optics

A box for a single photon

Philippe Grangier

The controlled manipulation of individual quantum objects, such as atoms, ions or photons, has developed considerably in recent years. A 'billiard ball' approach to individual atoms has been popularized by the fantastic landscapes created and explored using atomic force microscopy techniques, which exploit the repulsive force between microscope tip and atomic sample. But many experiments about the wave nature of matter, or about the particle nature of light, remind us that the fundamental nature of microscopic objects obeys the laws of quantum mechanics. A single photon provides the most striking evidence that a quantum particle is something much more elusive than a billiard ball. A new experiment reported on page 239 of this issue[1] demonstrates how to store a single photon, and, more importantly, how to watch it repeatedly.

As far as the position and momentum of particles are concerned, Heisenberg's well-known 'uncertainty relation' claims that both cannot be known simultaneously with perfect accuracy. A related idea is that a precise measurement in the microscopic world is not possible without introducing a perturbation, or 'back action', inherent in all measurements. For example, a very precise measurement of a particle's position will greatly disturb the particle's momentum and vice versa. This can be generalized to any pair of 'non-compatible' physical quantities, represented in quantum language as operators A and B. Although the precision in a single measurement of A is not restricted, the large fluctuations induced in B when measuring A may eventually couple back to A, which will then also be perturbed, making it difficult to perform repeated or continuous measurements. In response to this problem the concept of 'quantum non-demolition' (QND) measurements was introduced in the 1970s, in which a measurement strategy is chosen that evades the undesirable back action[2]. The key issue is to devise a measurement scheme so that the back-action 'noise' is kept entirely within unwanted observables. The quantity of interest then remains uncontaminated by the measurement process, allowing repeated measurements to be performed with arbitrarily high accuracy.

When the quantity to be monitored is the number of light particles — that is, the number of photons — a QND measurement is the best way to proceed. In the optical domain, QND experiments have already been used to explore the ultimate limit on the non-destructive extraction of information encoded in a laser beam[3]. The relevant Heisenberg relation is the so-called number–phase inequality, which sets a lower limit on the product of the dispersion ΔN (in the number of photons, N) and the dispersion $\Delta\phi$ (in the phase of the light wave, ϕ), such that $\Delta N \Delta\phi \geq 1/2$. In optical QND experiments, N is a very large number (so that $N \gg \Delta N \gg 1$) and $\Delta\phi \ll 1$. Although it is not possible to resolve individual photon numbers, it can be shown[3] that that the sensitivity of the measurement enters the quantum regime when ΔN is smaller than the 'shot-noise limit', $N^{1/2}$. To go beyond this 'large number' situation, experimentalists have to achieve single-photon resolution (that is, $\Delta N < 1$), allowing them to watch individual photons. Such experiments require extremely strong coupling between the measured 'signal' light field and another quantum system, usually called the 'meter', which reads out the number of photons without perturbing the signal.

This challenge has been met by a group working at the Ecole Normale Supérieure (ENS) in Paris[1], using the experimental techniques of cavity quantum electrodynamics (cavity QED). Here the 'signal' system is a microwave field confined within a niobium cavity, which is cooled by liquid helium to make it supraconducting and thereby increasing the storage time of photons in the cavity up to one millisecond. The 'meter' system is made of rubidium atoms that cross the cavity one at a time, and therefore pick up information about the light field (see Fig. 1). Ideally, according to the basic requirement for QND measurements, there should be no exchange of energy between the signal and meter. This can be obtained by having the frequency of light different from that of the rubidium atomic transition. In this 'non-resonant' situation the exchange of information is purely dispersive, that is, the atomic wavefunction only picks up a phase shift,

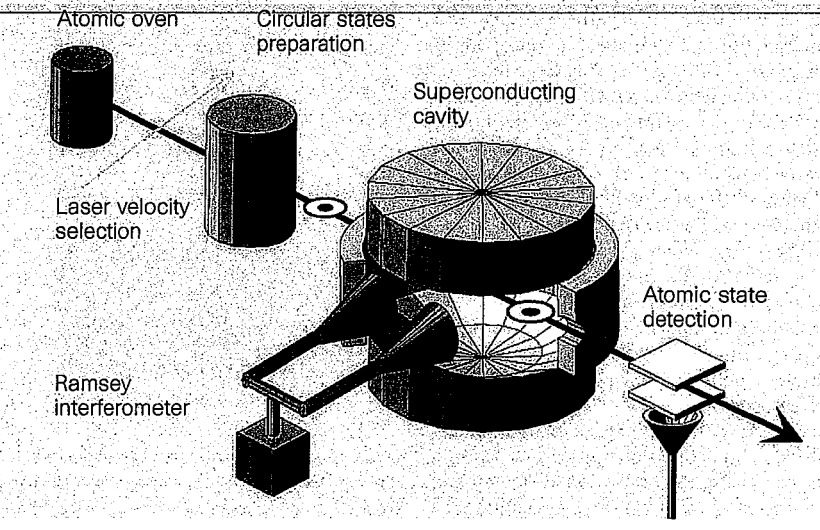

Figure 1 **How to detect a single photon repeatedly without destroying it. The photons used by Nogues *et al.*[1] are stored in the cavity (red) in the centre of the figure. The ring (yellow) between the two mirrors is cut open to reveal the inside of the 'photon-box'. Using lasers, rubidium atoms travelling along the main arrow are prepared in an appropriate state for interacting with the cavity field. These atoms (in 'circular' Rydberg states) have a very long lifetime, well suited for the experiment. The velocity selection and pulsed excitation scheme allows the position of each atom to be known. The Ramsey interferometer (green) is coupled to the inside of the photon box through holes in the ring (not shown). Combined with the detector (grey) it measures the phase of the atomic wavefunction. The value of this phase tells you whether the cavity contains zero or one photon.**

which is proportional to the number of photons in the cavity. Such a scheme was proposed a few years ago by the ENS group[4], but it has not been implemented yet, because the fact that the atom–field interaction is non-resonant makes it very weak. In the present experiment[1], a different trick is used: the interaction is fully resonant and thus much larger. An energy exchange does occur, but the parameters are chosen so that this energy exchange is fully reversible.

To understand how this exchange happens, we need to look briefly at concepts developed in the field of cavity QED. To cut a long story short, cavity QED uses optical or microwave resonators designed in such a way that the 'electric field per photon' is extremely large. Consequently, the coupling rate between an atom and the field is also very large, much larger than the dissipative effects caused by spontaneous emission from the atom, or the electric field leaking out of the cavity. So when the atom is within the cavity, the system can be described by only considering the coherent coupling between the atom and the cavity under various conditions. If there is no photon in the cavity, nothing happens; if there is one photon in the cavity, it is coherently absorbed and re-emitted by the atom before it leaves the cavity. In the latter case, the net energy exchange is zero, but it can be shown that because of this 'Rabi cycle' a phase shift occurs in the atomic wavefunction. Finally, if there is more than one photon, more Rabi cycles will occur, but this case can be ignored by the experimenters.

If one considers only the cases where the cavity is initially in an arbitrary quantum superposition, or mixture, of zero-photon and one-photon states, it is clear that this set-up will behave in a QND way. The phase information is extracted from the 'meter' atom using an interference effect, which transforms the phase shift into a detectable change in the atomic level. In fact, several schemes have been used by the ENS team[1]: either a first atom is used to deposit one photon within the cavity and a second atom detects it; or both atoms perform two successive measurements of a weak initial field, repeatedly allowing the experimenter to know whether the cavity contains zero photons or one photon.

The ENS format[1] cannot easily be generalized to higher photon numbers (this would require using the non-resonant interaction described above), but it is worth pointing out that the techniques that yield this single-photon QND measurement may also generate other interesting effects. The fact that one photon can significantly shift the atomic phase is the key to building a quantum logic gate, suggesting a route to quantum computing[5]. It can be expected that this experiment will open the way to many other ones, which will explore further the very peculiar rules for writing in and reading out the information encoded in quantum objects. □

Philippe Grangier is at the Institut d'Optique, BP 147-F91403, Orsay, France.
e-mail: philippe.grangier@iota.u-psud.fr

1. Nogues, G. *et al. Nature* **400**, 239–242 (1999).
2. Braginsky, V. B., Vorontsov, Y. L. & Thorne, K. S. *Science* **209**, 547–557 (1980).
3. Grangier, P., Levenson, J. A. & Poizat, J.-P. *Nature* **396**, 537–542 (1998).
4. Brune, M., Haroche, S., Lefévre, V., Raimond, J. M. & Zagury, N. *Phys. Rev. Lett.* **65**, 976–979 (1990).
5. Deutsch, D. & Ekert, A. *Physics World* 47–52 March (1998).

Neurobiology

Monkeys play the odds

M. James Nichols and William T. Newsome

On a sunny, spring morning, an experienced fisherman furrows his brow and weighs the merits of one fishing hole against another further upstream. At both sites he sees promising signs, and a novice could not distinguish between the two. But the veteran knows that, on mornings like this, bigger fish bite more often upstream — and he selects the upstream spot.

Like the fisherman we all make countless day-to-day decisions — selecting restaurants, betting in office football pools, buying used cars, and so on. We base these decisions not just on current information, but also on accumulated experience and expectations about the likelihood and size of rewards. Experimental evidence indicates that animals also shape their behaviour based on the expected size and probability of rewards. Indeed, economists[1–4], psychologists[5–8] and ecological biologists[9,10] place these critical variables at the centre of models about human and animal decision-making.

Platt and Glimcher (reporting on page 233 of this issue)[11] have now applied decision theory to combined behavioural and neurophysiological experiments in rhesus monkeys, providing new insights into how decision variables are represented in the central nervous system. Despite the importance of reward expectations in shaping behaviour, neurophysiologists have largely ignored them in studies of brain function (but see Gallistel[5]). Instead, they have adopted a framework in which particular patterns of

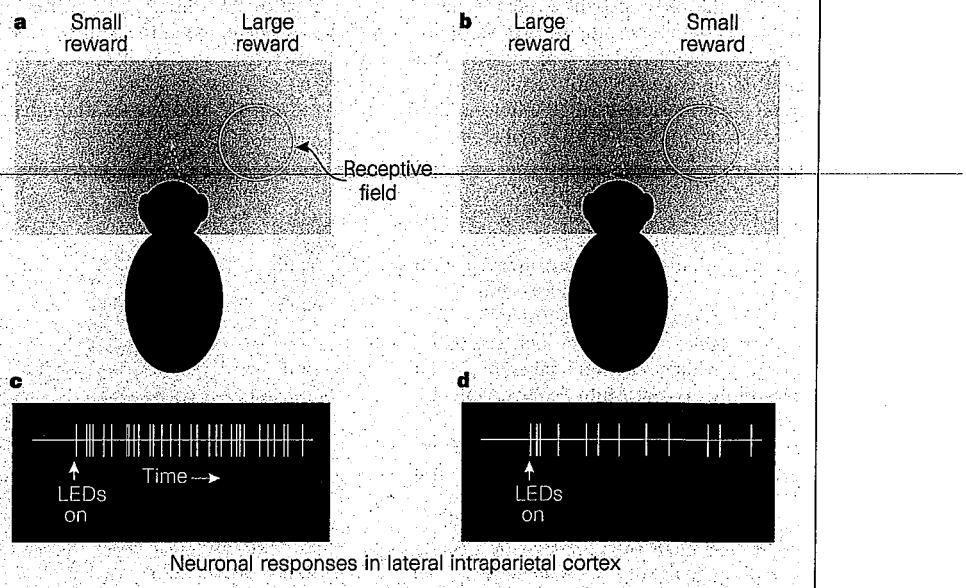

Figure 1 **Assessing neural correlates of decision making. In a simple decision-making task devised by Platt and Glimcher[11], a monkey sits facing a viewing screen. On each trial, he first looks at a central fixation point (yellow cross). Then, two light-emitting diodes (LEDs; yellow circles) are illuminated at different locations on the viewing screen, one inside the receptive field (white circle) of the neuron under study, the other outside. After a delay, the fixation point is extinguished and the monkey receives a juice reward for looking to either of the two LEDs. a, In some blocks of trials, the LED within the receptive field is associated with a larger reward. b, In other blocks, the same LED is associated with a smaller reward. c,d, Schematized neuronal responses to the onset of the LED in the receptive field for the two reward conditions depicted in panels a and b. Vertical hatch marks indicate action potentials after illumination of the LEDs (vertical arrow). This hypothetical neuron discharges more vigorously for the same visual stimulus in its receptive field when the stimulus is associated with a larger juice reward.**

If the atomic frequency is detuned from the cavity mode by $\delta/2\pi$ with $|\delta| \geq \Omega_0$, emission and absorption of photons by the probe atoms are suppressed owing to the adiabatic variation of $\Omega(z)$ when the atom crosses the gaussian cavity mode (see Methods). The atom–field coupling results in shifts of the atomic and cavity frequencies[9]. The atomic shift depends on the field intensity and thus provides QND information on the photon number n. Following a proposal made in refs 14 and 15, our aim is to read this information by an interferometric method and to monitor the jumps of n between 0 and 1 under the effect of thermal fluctuations and relaxation in the cavity.

Before entering C, the atoms are prepared in a superposition of e and g by a classical resonant field in the auxiliary cavity R_1 (see Fig. 1). During the atom–cavity interaction, this superposition accumulates a phase $\Phi(n,\delta)$. The atomic coherence at the exit of C is probed by subjecting the atoms to a second classical resonant field in R_2, before detecting them in the state-selective counter D. The combination of R_1, R_2 and D is a Ramsey interferometer. The probability of detecting the atom in g is a sine function of the relative phase of the fields in R_1 and R_2. This phase is adjusted so that the atom is ideally found in g if C is empty ($n = 0$). The detuning $\delta/2\pi$ is set at 67 kHz, corresponding to $\Phi(1,\delta) - \Phi(0,\delta) = \pi$. As a result, the atom is found in e if $n = 1$. As long as the probability of finding more than one photon remains negligible, e thus codes for the one-photon state, $|1\rangle$, and g for the vacuum, $|0\rangle$. The probability of finding two photons in a thermal field at $T = 0.8$ K is only 0.3%, and may be neglected in a first approximation.

We first monitor the field fluctuations in C. Figure 2a (top trace) shows a 2.5 s sequence of 2,241 detection events, recording the birth, life and death of a single photon. At first, atoms are predominantly detected in g, showing that C is in $|0\rangle$. A sudden change from g to e in the detection sequence at $t = 1.054$ s reveals a jump of the field intensity, that is, the creation of a thermal photon, which disappears at $t' = 1.530$ s. This photon has survived 0.476 s (3.7 cavity lifetimes), corresponding to a propagation of about 143,000 km between the cavity mirrors.

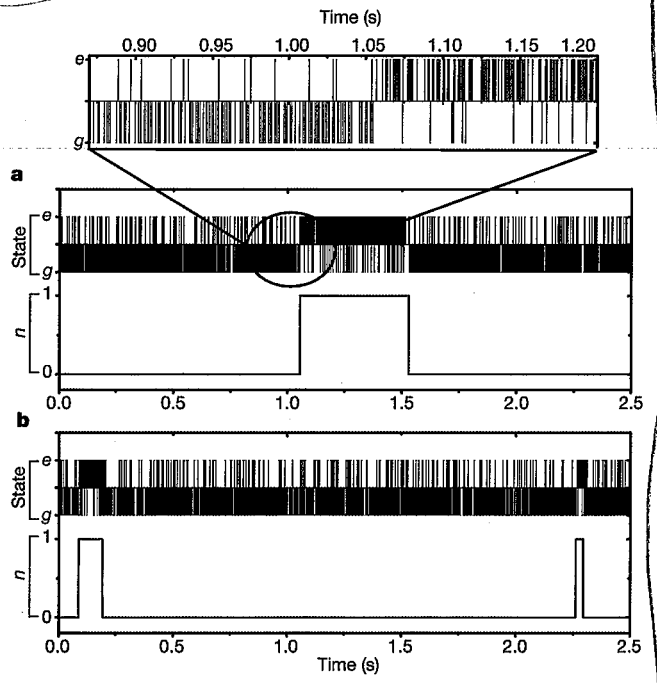

Figure 2 | Birth, life and death of a photon. **a**, QND detection of a single photon. Red and blue bars show the raw signal, a sequence of atoms detected in e or g, respectively (upper trace). The inset zooms into the region where the statistics of the detection events suddenly change, revealing the quantum jump from $|0\rangle$ to $|1\rangle$. The photon number inferred by a majority vote over eight consecutive atoms is shown in the lower trace, revealing the birth, life and death of an exceptionally long lived photon. **b**, Similar signals showing two successive single photons, separated by a long time interval with cavity in vacuum.

The inset in Fig. 2a zooms into the detection sequence between times $t_1 = 0.87$ s and $t_2 = 1.20$ s, and displays more clearly the individual detection events. Imperfections reduce the contrast of the Ramsey fringes to 78%. There is a $p_{g|1} = 13\%$ probability of detecting an atom in g if $n = 1$, and a $p_{e|0} = 9\%$ probability of finding it in e if $n = 0$. Such misleading detection events, not correlated to real photon number jumps, are conspicuous in Fig. 2a and in its inset. To reduce their influence on the inferred n value, we apply a simple error correction scheme. For each atom, n is determined by a majority vote involving this atom and the previous seven atoms (see Methods). The probabilities for erroneous $n = 0$ ($n = 1$) photon number assignments are reduced below 1.4×10^{-3} (2.5×10^{-4}) respectively per detected atom. The average duration of this measurement is 7.8×10^{-3} s, that is, $T_c/17$. The bottom trace in Fig. 2a shows the evolution of the reconstructed photon number. Another field trajectory is presented in Fig. 2b. It displays two single-photon events separated by a 2.069 s time interval during which C remains in vacuum. By probing the field non-destructively in real time, we realize a kind of 'Maxwell demon', sorting out the time intervals during which the thermal fluctuations are vanishing.

Analysing 560 trajectories, we find an average photon number $n_0 = 0.063 \pm 0.005$, slightly larger than $n_t = 0.049 \pm 0.004$, the thermodynamic value at the cavity mirror temperature, 0.80 ± 0.02 K. Attributing the excess photon noise entirely to a residual heating of the field by the atomic beam yields an upper bound to the emission rate per atom of 10^{-4}. This demonstrates the efficient suppression of atomic emission due to the adiabatic variation of the atom–field coupling. This suppression is a key feature that makes possible many repetitions of the QND measurement. Methods based on resonant phase shifts have much larger emission rates, in the 10^{-1} range per atom[3]. Non-resonant methods in which the detector is permanently coupled to the cavity[12] have error rates of the order of Ω_0^2/δ^2, and would require much larger δ/Ω_0 ratios to be compatible with the observation of field quantum jumps.

In a second experiment, we monitor the decay of a single-photon Fock state prepared at the beginning of each sequence. We initialize the field in $|0\rangle$ by first absorbing thermal photons with ~10 atoms prepared in g and tuned to resonance with the cavity mode (residual photon number $\sim 0.003 \pm 0.003$). We then send into the cavity a single atom in e, also resonant with C. Its interaction time is adjusted so that it undergoes half a Rabi oscillation, exits in g and leaves C in $|1\rangle$. The QND probe atoms are then sent across C. Figure 3a shows a typical single photon trajectory (signal inferred by the majority vote) and Fig. 3b–d presents the averages of 5, 15 and 904 such trajectories. The staircase-like feature of single events is progressively smoothed out into an exponential decay, typical of the evolution of a quantum average.

We have neglected so far the probability of finding two photons in C. This is justified, to a good approximation, by the low n_0 value. A precise statistical analysis reveals, however, the small probability of two-photon events, which vanishes only at 0 K. When C is in $|1\rangle$, it decays towards $|0\rangle$ with the rate $(1 + n_0)/T_c$. This rate combines spontaneous ($1/T_c$) and thermally stimulated (n_0/T_c) photon annihilation. Thermal fluctuations can also drive C into the two-photon state $|2\rangle$ at the rate $2n_0/T_c$ (the factor of 2 is the square of the photon creation operator matrix element between $|1\rangle$ and $|2\rangle$). The total escape rate from $|1\rangle$ is thus $(1 + 3n_0)/T_c$, a fraction $2n_0/(1 + 3n_0) \approx 0.10$ of the quantum jumps out of $|1\rangle$ being actually jumps towards $|2\rangle$.

In this experiment, the detection does not distinguish between $|2\rangle$ and $|0\rangle$. The incremental phase shift $\Phi(2,\delta) - \Phi(1,\delta)$ is 0.88π for $\delta/2\pi = 67$ kHz . The probability of detecting an atom in g when C is in $|2\rangle$ is ideally $[1 - \cos(0.88\pi)]/2 = 0.96$, indistinguishable from 1 within the experimental errors. Since the probability for $n > 2$ is